Electromagnetically induced grating with Rydberg atoms

Sobia Asghar,[1] Ziauddin,[1,*] Shahid Qamar,[2] and Sajid Qamar[1,†]

[1]*Quantum Optics Lab, Department of Physics, COMSATS Institute of Information Technology, Islamabad 45550, Pakistan*

[2]*Department of Physics and Applied Mathematics, Pakistan Institute of Engineering and Applied Sciences, Nilore, Islamabad 45650, Pakistan*

(Received 29 April 2016; revised manuscript received 27 July 2016; published 13 September 2016)

We present a scheme to realize electromagnetically induced grating in an ensemble of strongly interacting Rydberg atoms, which act as superatoms due to the dipole blockade mechanism. The ensemble of three-level cold Rydberg-dressed (^{87}Rb) atoms follows a cascade configuration where a strong standing-wave control field and a weak probe pulse are employed. The diffraction intensity is influenced by the strength of the probe intensity, the control field strength, and the van der Waals (vdW) interaction. It is noticed that relatively large first-order diffraction can be obtained for low-input intensity with a small vdW shift and a strong control field. The scheme can be considered as an amicable solution to realize the atomic grating at the microscopic level, which can provide background- and dark-current-free diffraction.

DOI: 10.1103/PhysRevA.94.033823

I. INTRODUCTION

In quantum optics and laser physics, coherence and interference play an important role and have been an important area of research [1]. A strong laser field can control the optical response of the medium by introducing quantum coherence in the system. Under suitable conditions, the absorption of the probe field vanishes, which is known as the phenomenon of electromagnetically induced transparency (EIT) [2,3]. The EIT phenomenon has a key role in nonlinear optics [4,5] and quantum information processing [6]. Interestingly, when the traveling wave of EIT is replaced by a standing wave, an atomic grating is formed which is known as electromagnetically induced grating (EIG) [7]. The amplitude of a resonant probe field, incident on EIG, changes in a period which is due to the spatial modulation induced by the standing wave. As a result, the probe field can be diffracted into the high-order directions. The EIG has been observed experimentally using an ultracold atomic medium [8].

The EIG and its applications have attracted researchers in various fields of science to study, for example, diffracting and switching a quantized probe field [9], probing the optical properties of a material [10], and all optical switching, routing, and light storage [11–13]. Moreover, different systems have been suggested for the study of EIG due to its tunability [14–20]. The grating with giant intensity of high-order diffraction has been studied using a three-level ladder type system [14]. Similarly, grating phenomena have been studied using double-dark-state atomic systems [10], spontaneously generated coherence [15], asymmetric quantum wells [16,17], and active Raman gain cold atoms [19].

One can notice that EIG is a background-free technique having no associated dark current as well [8]. However, due to its quantum mechanical nature, the main drawback is its practical implementation; microscopic quantum objects are essential to realize quantum mechanical processing for practical implementation. An amicable solution can be to use Rydberg atoms. Rydberg atoms, which exhibit a long radiative lifetime and strong dipole-dipole or van der Waals (vdW) interactions, have already been considered to observe EIT [21–25].

Strong dipole-dipole interactions between Rydberg atoms can block all but a single optical excitation in a volume of several micrometers [26–28]. This transforms N number of atoms within this volume to one collective two-level atomic system called a *superatom*, which can be used for the coherent manipulation and entanglement of collective excitations in mesoscopic ensembles of cold Rydberg atoms [26]. The dipole blockade mechanism, in which atoms in a Rydberg state suppress the excitation of more than one Rydberg state of neighboring atoms within a certain specific volume [26,29], makes the Rydberg atoms striking candidates for single-photon quantum devices [30,31].

In this article, we suggest EIG via Rydberg atoms. The motivations come from a recent study [32] where Rydberg-dressed EIT systems in a three-level cascade configuration have been proposed and the transparency window has been controlled via the strength of the probe field. This theoretical model is based on coarse-grained treatment of the atomic medium consisting of superatoms (SAs) and employs collective states of the atoms in the blockade volume that have only one Rydberg excitation. The EIT phenomenon has been explained with SAs in the mean field with two-photon correlation for the nonlinear response to Rydberg excitation [32,33]. We extend the idea to realize EIG with Rydberg atoms and consider a medium consisting of a large number of SAs and each SA contains an ensemble of three-level atoms having a cascade configuration with only one atom in the Rydberg state. The medium acts as EIG in the presence of a standing-wave field, whereas diffraction of a weak probe field, which is incident on the EIG, is calculated. We observe that maximum diffraction intensity is achievable for low-input intensity and small values of vdW interactions.

II. MODEL

We consider an ensemble of N numbers of SAs, where each SA contains a cold atomic medium in volume V interacting with two fields. In each SA only one atom is in a Rydberg state while all other Rydberg excitations are suppressed by the

*ziauddin@comsats.edu.pk

†sajid_qamar@comsats.edu.pk

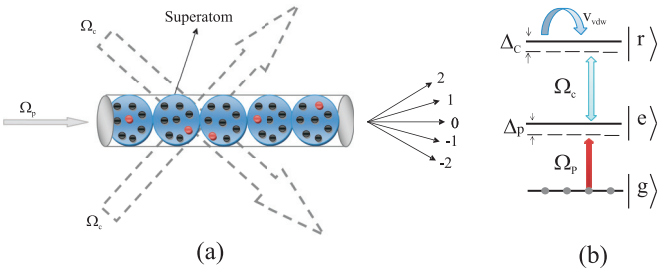

FIG. 1. (a) Schematics of the superatoms, with one Rydberg state $|r\rangle$ interacting with probe and control (standing-wave) fields. (b) Energy-level configuration for a three-level cascade atomic system.

dipole blockade mechanism. A weak probe light beam and a position-dependent coupling field (which form a standing wave) drive the atomic medium as depicted in Fig. 1(a). Here the length of the interaction region which experiences the probe field is assumed to be L. Under the slowly varying approximation and the steady-state regime, the propagation of the probe field using Maxwell's equation can be written as [7,19]

$$\frac{\partial E_p}{\partial z} = [\alpha + i\beta]E_p, \tag{1}$$

where α and β are the absorption and dispersion coefficients of the probe field, respectively, and are related by the dielectric susceptibility of the medium by $\alpha(x) = [\frac{2\pi}{\lambda}]\mathrm{Im}[\chi]$ and $\beta(x) = [\frac{2\pi}{\lambda}]\mathrm{Re}[\chi]$, whereas χ is the dielectric susceptibility of the atomic medium. For simplification and focus on characteristics of EIG, the transverse part of Eq. (1) has been ignored [7,19]. The transmission function of the probe field at $z = L$ can easily be calculated analytically using Eq. (1) and is given by

$$T(x) = e^{-\alpha(x)L + i\beta(x)L}, \tag{2}$$

where the terms $e^{-\alpha(x)L}$ and $e^{i\beta(x)L}$ are associated with absorption and phase modulation, respectively.

Assuming that the input probe field is a plane wave [7,19], the diffraction intensity distribution can be expressed as

$$I(\theta) = |E(\theta)|^2 \times \frac{\sin^2(N\pi\Lambda_x \sin(\theta)/\lambda)}{N^2 \sin^2(\pi\Lambda_x \sin(\theta)/\lambda)}, \tag{3}$$

where N is the number of the spatial period of the atomic grating, θ is the diffraction angle along the z direction, and the parameter Λ_x is the spatial period in the x direction, which is equal to $[\frac{\pi}{k_x}]$, whereas the term $E(\theta)$ is the Fourier transform of $T(x)$ and describes the Fraunhofer diffraction of a single space period as

$$E(\theta) = \int_0^1 T(x) e^{-2\pi i \Lambda_x x \sin(\theta)/\lambda} dx. \tag{4}$$

Since we are interested in the nth-order diffraction intensity next we calculate $I(\theta_n)$ along the n-order diffraction angle established by the grating equation, the diffraction order n is defined as $n = (\frac{\Lambda_x \sin(\theta)}{\lambda})$, where $n = 0, 1, 2, 3,...$for zeroth order, first order, and so on. The expression of nth-order diffraction intensity is

$$I(\theta_n) = |E(\theta_n)|^2, \tag{5}$$

$$E(\theta_n) = \int_0^1 T(x) e^{-2\pi i n x} dx. \tag{6}$$

III. ATOM-FIELD INTERACTION

We consider an ensemble of cold ^{87}Rb atoms with energy levels $|g\rangle \equiv 5S_{1/2}|F = 2, m_F = 2\rangle$, $|e\rangle \equiv 5P_{3/2}|F = 3, m_F = 3\rangle$, and $|r\rangle \equiv 60S_{1/2}$ interacting with a probe pulse and a standing-wave control field in a cascade atom-field configuration [see Fig. 1(b)]. Each atom has energy levels $|g\rangle$, $|e\rangle$, and $|r\rangle$. The probe field of the frequency ω_p drives the transition between $|g\rangle$ and $|e\rangle$ with the Rabi frequency Ω_p, whereas the standing-wave control field with the Rabi frequency $\Omega_c(x) = \Omega_1 \sin[\frac{\pi x}{\Lambda_x}]$ drives the transition between $|r\rangle$ and $|e\rangle$. The control field excites the atoms to the Rydberg state $|r\rangle$ and the atoms interact with each other via a vdW potential, $|\Delta(\mathbf{r}_i - \mathbf{r}_j) = C_6/|\mathbf{r}_i - \mathbf{r}_j|^6$ [32], where $\mathbf{r}_i$ and $\mathbf{r}_j$ are the positions of the ith and jth atoms, respectively. We can write the total Hamiltonian for our system as

$$H = H_a + H_{af} + H_{\mathrm{vdW}}, \tag{7}$$

where

$$\begin{aligned} H_a &= -\hbar \sum_j^N \left[\Delta_p \sigma_{ee}^j + \Delta_2 \sigma_{rr}^j\right], \\ H_{af} &= -\hbar \sum_j^N \left[\Omega_p \sigma_{eg}^j + \Omega_c(x)\sigma_{re}^j + \mathrm{H.c.}\right], \\ H_{\mathrm{vdW}} &= \hbar \sum_{i<j}^N \sigma_{rr}^i \Delta(\mathbf{r}_i - \mathbf{r}_j)\sigma_{rr}^j, \end{aligned} \tag{8}$$

whereas $\Delta_p = \omega_p - \omega_{eg}$, $\Delta_c = \omega_c - \omega_{re}$, and $\Delta_2 = \Delta_p + \Delta_c$ is the two-photon detuning and $\sigma_{\alpha\beta}^j = |\alpha\rangle_{jj}\langle\beta|$ is the transition operator for the jth atom at position $\mathbf{r}_j$. Using the Hamiltonian, Eq. (7), we can write down the Heisenberg Langevin equations as

$$\begin{aligned} \dot{\sigma}_{gg}^j &= i\Omega_p^* \sigma_{ge}^j - i\Omega_p \sigma_{eg}^j + \Gamma_e \sigma_{ee}^j, \\ \dot{\sigma}_{ee}^j &= i\Omega_p \sigma_{eg}^j - i\Omega_p^* \sigma_{ge}^j - i\Omega_c(x)\sigma_{re}^j - i\Omega_c^*(x)\sigma_{er}^j \\ &\quad + \Gamma_r \sigma_{rr}^j - \Gamma_e \sigma_{ee}^j, \\ \dot{\sigma}_{ge}^j &= (i\Delta_p - \gamma_{ge})\sigma_{ge}^j + i\Omega_p\left(\sigma_{gg}^j - \sigma_{ee}^j\right) + i\Omega_c^*(x)\sigma_{gr}^j, \\ \dot{\sigma}_{gr}^j &= \{i[\Delta_2 - S(\mathbf{r})] - \gamma_{gr}\}\sigma_{gr}^j + i\Omega_c(x)\sigma_{ge}^j - i\Omega_p \sigma_{er}^j, \\ \dot{\sigma}_{er}^j &= i(\Delta_p - S(\mathbf{r}) - \gamma_{er})\sigma_{er}^j - i\Omega_p^* \sigma_{gr}^j + i\Omega_c(x)\left[\sigma_{ee}^j - \sigma_{rr}^j\right], \end{aligned} \tag{9}$$

where Γ_e is the atomic decay rate and γ_{ge}, γ_{er}, and γ_{gr} are the dephasing rates. Because the Rydberg state exhibits a longer lifetime, therefore $\gamma_{ge} \gg \gamma_{gr}$. Here, $S(\mathbf{r})$ is the vdW-force-induced shift of the Rydberg state $|r\rangle$ for an atom at position $\mathbf{r}$

and can be defined as

$$S(\mathbf{r}) = \sum_{i<j}^{n_{SA}} \Delta(\mathbf{r} - \mathbf{r}_j)\sigma_{rr}, \tag{10}$$

where $\Delta(\mathbf{r} - \mathbf{r}_j)$ is the vdW potential at position $\mathbf{r}$ and σ_{rr} is the population of the Rydberg state.

The steady-state solution of Eq. (9) can be calculated as

$$\sigma_{ge} = \frac{i[\gamma_{gr} - i(-S(\mathbf{r}) + \Delta_2)]\Omega_p}{(\gamma_{ge} - i\Delta_p)[\gamma_{gr} - i(-S(\mathbf{r}) + \Delta_2)] + \Omega_c^2(x)},$$
$$\sigma_{gr} = -\frac{\Omega_c(x)\Omega_p}{(\gamma_{ge} - i\Delta_p)[\gamma_{gr} - i(-S(\mathbf{r}) + \Delta_2)] + \Omega_c^2(x)}. \tag{11}$$

Following the same approach as described in Ref. [32] and considering the stationary-state solution of Eq. (9) without the vdW shift $S(\mathbf{r})$, the population of Rydberg state can be defined as

$$\langle\sigma_{rr}\rangle = \sigma_{rg}\sigma_{gr}, \tag{12}$$

By considering $\gamma_{rg} \ll \gamma_{eg}$ and $\Delta_p < \gamma_{eg}$, the population of the Rydberg state $|r\rangle$ can be calculated as

$$\langle\sigma_{rr}\rangle \approx \frac{|\Omega_c(x)|^2|\Omega_p|^2}{|\Omega_c(x)|^4 + \Delta_2^2\gamma_{ge}^2}. \tag{13}$$

Next, we consider a vdW-induced shift for the medium consisting of a collection of superatoms and therefore we replace σ_{rr} with the new variable Σ_{RR}. Further, we consider that the atom in the Rydberg state induces the vdW shift $\Delta(R)$ to another atom located at a distance, R. The vdW interaction suppresses the excitation of all the atoms in a small volume, V_{SA}, which is known as a Rydberg blockade or SA [26]. The number of atoms in a SA may be defined as $n_{SA} = \rho(\mathbf{r})V_{SA}$, where $\rho(\mathbf{r})$ is the atomic density. There is only one Rydberg excited atom in each SA, i.e., in V_{SA}. The total medium can then be treated as a collection of SAs, and the number of superatoms within the volume V can be defined as $N_{SA} = \rho_{SA}V$. The total vdW shift at position $\mathbf{r}$ can thus be written as

$$S(\mathbf{r}) = \sum_{j}^{N_{SA}} \Delta(\mathbf{r} - \mathbf{r}_j)\Sigma_{RR}(\mathbf{r}_j) = \bar{\Delta}\Sigma_{RR}(\mathbf{r}) + s(\mathbf{r}), \tag{14}$$

where the first term in the right-hand side of Eq. (14) shows the excited SA at $\mathbf{r}_j = r$, i.e., $\Sigma_{RR}(\mathbf{r}) \to 1$, which induces a divergent vdW shift in a volume of SA, and then $\bar{\Delta}(0) \cong \frac{1}{V_{SA}}\int_{V_{SA}} \Delta r' d^3r' \to \infty$. The second part in right-hand side of Eq. (14) shows the vdW shift induced due to the external SAs outside the volume and can be expressed as $s(\mathbf{r}) = \sum_{j\neq j_r}^{N_{SA}} \Delta(\mathbf{r} - \mathbf{r}_j)\Sigma_{RR}(\mathbf{r}_j)$. We can calculate the expression for $s(\mathbf{r})$ by replacing the summation by integration over the total volume and using the mean-field approximation as discussed in Ref. [32]:

$$\langle s(\mathbf{r})\rangle = \frac{w}{8}\langle\Sigma_{RR}(\mathbf{r})\rangle, \tag{15}$$

where w is the half-width of the Lorentzian function of the population in a Rydberg state given by $\frac{|\Omega_c|^2}{\gamma_e}$. To find the analytical expression for $s(\mathbf{r})$, we need to calculate $\Sigma_{RR}(\mathbf{r})$. The dynamics of individual SAs can be described in the form of collective states and operators within the blockade volume such that the ground state and the single collective Rydberg excited state are given by

$$|G\rangle = |g_1, g_2, g_3, \ldots, g_{n_{SA}}\rangle, \tag{16}$$

and

$$|R^{(1)}\rangle = \frac{1}{\sqrt{n_{SA}}}\sum_{j}^{n_{SA}} |g_1, g_2, g_3, \ldots, r_j, \ldots, g_{n_{SA}}\rangle. \tag{17}$$

For a single-atom treatment and considering the SA in the ground state $|G\rangle$, the total population of the Rydberg state $\Sigma_{RR}(\mathbf{r})$ can be defined as [32]

$$\Sigma_{RR} = \Sigma_{RG}\Sigma_{GR}, \tag{18}$$

which replaces Eq. (12), where

$$\Sigma_{GR} = \frac{\sqrt{n_{SA}}\Omega_c(x)\Omega_p\Sigma_{GG}}{\Delta_2(i\gamma_{eg} + \Delta_p) - |\Omega_c(x)|^2}. \tag{19}$$

Using Eqs. (18) and (19) and $\Sigma_{GG} + \Sigma_{RR} = 1$, the final expression for Σ_{RR} can take the form

$$\Sigma_{RR} = \frac{n_{SA}|\Omega_c(x)|^2|\Omega_p|^2}{|\Omega_c(x)|^2|\Omega_p|^2 n_{SA} + [\Delta_2\Delta_p - |\Omega_c(x)|^2]^2 + \gamma_{eg}^2\Delta_2^2}. \tag{20}$$

Looking through Eqs. (14) to (20), it can be realized that Rydberg blockade makes the medium nonlinear where the Rydberg blockade effect comes from the vdW-induced shift and is directly related to Σ_{RR}. Here, Σ_{RR} depends on the input-probe-field Rabi frequency Ω_p and if there is no vdW-induced shift in the medium then $s(r) = 0$ and the medium is no longer dependent on the input-probe-field intensity. The realization of EIG in the present work is to control the diffracted intensity via the probe field and we can increase or decrease the diffracted intensity via control of the probe field.

Finally, the optical susceptibility of the proposed atomic medium can therefore be calculated as

$$\chi = \xi\left[\Sigma_{RR}\frac{i\gamma_{eg}}{\gamma_{eg} - i\Delta_p} + [1 - \Sigma_{RR}] \times \frac{i\gamma_{eg}}{\gamma_{eg} - i\Delta_p + |\Omega_c(x)|^2[\gamma_{rg} - i(\Delta_2 - \langle s\rangle)]^{-1}}\right], \tag{21}$$

where $\xi = \frac{2N_{SA}|\mu_{eg}|^2}{\hbar\epsilon_0}$. The interaction length can be defined in units of $\eta = [\frac{\lambda}{2\pi\xi}]$. From Eq. (20), it is clear that Σ_{RR} depends on n_{SA} which is directly related to the superatoms. The blockade effects arise from the dipole-dipole interactions between atoms. Thus, the dipole blockade affects the susceptibility of the system as shown in Eq. (20). For the case when the blockade effect is so strong, i.e., $\Sigma_{RR} \to 1$, the probe field sees a two-level absorbing system. On the contrary, for noninteracting atoms, i.e, $\Sigma_{RR} \to 0$, the whole system reduces to a single three-level EIT configuration.

IV. RESULTS AND DISCUSSION

We start analysis of our proposed model for the EIG via Rydberg atoms by studying the behavior of the transmission function corresponding to the incident probe light. We plot the magnitude of the transmission function $|T(x)|$ versus spatial

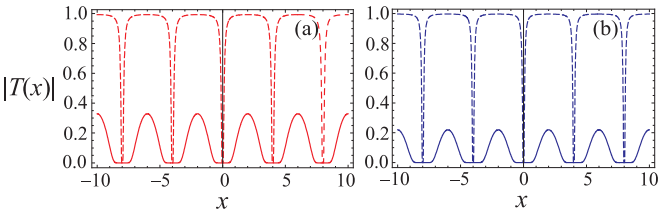

FIG. 2. Transmission function $T(x)$ versus transverse position x: (a) For $\Omega_p = 0.5\gamma$ (solid curve) and $\Omega_p = 0.005\gamma$ (dashed curve) while $\Omega_1 = 30\gamma$, and (b) for $\Omega_1 = 2\gamma$ (solid curve) and $\Omega_1 = 30\gamma$ (dashed curve) while $\Omega_p = 0.005\gamma$. The common parameters are $N = 5$, $\gamma = 1$ MHz, $n_{\rm SA} = 20$, $L = 200\eta$, $\Delta_p = \Delta_c \approx 0$, $\gamma_{eg} = 3\gamma$, and $\gamma_{rg} = 0.01\gamma$.

period x using Eq. (2) for different intensities of the probe and control fields. The plots show nodes and antinodes of the standing-wave field at the transmission locations (see Fig. 2). To study the effect of the probe field on transmission through the EIG, we plot $|T(x)|$ versus x for Ω_p equal to 0.5γ (solid line) and 0.005γ (dashed line) while keeping the control-field Rabi frequency constant, i.e., $\Omega_1 = 30\gamma$ [see Fig. 2(a)]. The other parameters are $N = 5$, $\gamma = 1$ MHz, $n_{\rm SA} = 20$, $L = 200\eta$, $\Delta_p = \Delta_c \approx 0$, $\gamma_{eg} = 3\gamma$, and $\gamma_{rg} = 0.01\gamma$. It can be noticed that at the transverse locations, around the antinodes, transmission increases with decreasing probe–field intensity. The probe-field absorption in this case is decreased and EIT is enhanced which is because for a high intensity of the probe field more than one photon per SA exists and excess photons are subjected to the enhanced absorption by the two-level atomic system [32]. Next to study the influence of the control field on transmission through the EIG, we plot $|T(x)|$ versus x for two different choices of the control-field Rabi frequency Ω_1, $\Omega_1 = 2\gamma$ (solid line) and $\Omega_1 = 30\gamma$ (dashed line), while now keeping the probe-field Rabi frequency constant, i.e., $\Omega_p = 0.005\gamma$, and the remaining parameters unchanged [see Fig. 2(b)]. The plot shows that the transmission increases at antinodes with the control-field intensity. It is in accordance with the EIT phenomenon, which depends on the control-field intensity, and the earlier observations [22,32].

In Fig. 3, we show a plot of the diffraction intensity $I(\theta)$ versus the diffraction angle θ while varying the incident probe-

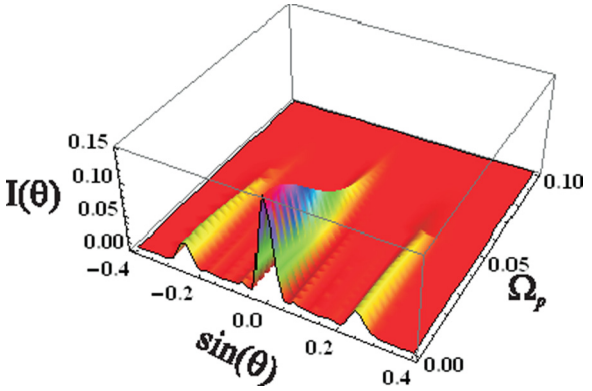

FIG. 3. Three-dimensional plot of the diffraction intensity $I(\theta)$ versus $\sin(\theta)$ and the probe-field Rabi frequency Ω_p. The other parameters are the same as those in Fig. 2.

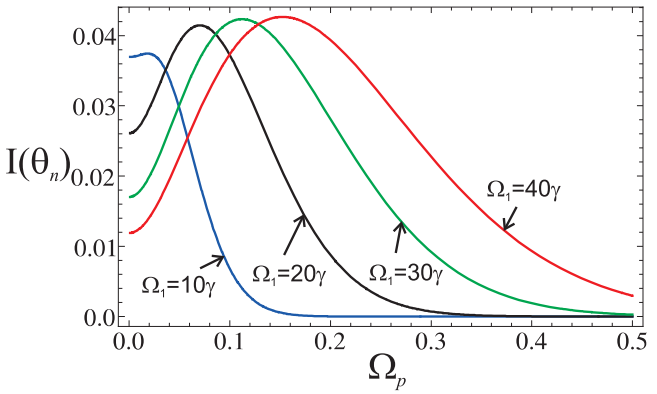

FIG. 4. (a) Plots of the first-order diffraction intensity $I(\theta_n)$ ($n = 1$) versus the probe-field intensity Ω_p for Ω_1 equal to 10γ (blue), 20γ (black), 30γ (green), and 40 γ(red). The remaining parameters are the same as those in Fig. 2.

field intensity. The three-dimensional plot shows the zeroth- and first-order diffraction at $\theta = 0$ and ± 0.25 rad, respectively; the remaining parameters are same as those in Fig. 2. The results are in good agreement with Fig. 2(a) and the diffraction intensity decreases as the probe-field Rabi frequency Ω_p increases. For small values of Ω_p, the medium encounters a linear EIT response, and as a result maximum diffraction intensity can be obtained. As Ω_p increases, the possibility of two or more than two photons excitation in Rydberg states $|r\rangle$ in the same superatom becomes higher, which suppresses the linear EIT response and then the medium behaves like an absorber. Therefore, the diffraction intensity decreases with increases in the probe-field intensity. We have already noticed that the transmission function $T(x)$ strongly depends on the probe as well as the control fields (see Fig. 2). Therefore, it is instructive to study the influence of the probe and the control field on first-order diffraction. We consider $\theta = 0.25$ rad and first-order diffraction ($n = 1$) and plot the diffraction intensity $I(\theta_n)$ versus the probe-field Rabi frequency for four different choices of the control-field Rabi frequency, i.e., Ω_1 is equal to 10γ, 20γ, 30γ, and 40γ (see Fig. 4). The behavior of the plots show that the first-order diffraction intensity $I(\theta_n)$, initially, increases with the probe-field Rabi frequency. However, the first-order diffraction intensity, after attaining a maximum value for a certain choice of the probe-field intensity which depends on the control-field intensity, decreases with a further increase in the probe-field intensity. These results are in agreement with the results presented in Fig. 2 and Ref. [32]. It is clear that the absorption of the probe field can be suppressed in the presence of strong control-field intensity and, therefore, slightly higher intensity in the first-order diffraction can be obtained via the control field even in the presence of a relatively large probe field. However, the overall behavior remains the same for all curves; i.e., after attaining the maximum value it decreases with a further increase in the probe-field Rabi frequency.

Further, we study the influence of the vdW shift $s(r)$ induced by the external SAs on the zeroth- and first-order diffraction intensities. As mentioned already, the vdW shift $s(r)$ is directly related to Σ_{RR}, which plays an important role in the susceptibility of the atomic system. When Σ_{RR}

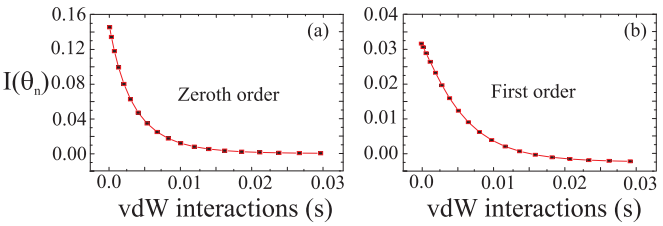

FIG. 5. Diffraction intensity versus vdW interactions (s) for (a) zeroth order ($n = 0$) and (b) first order ($n = 1$). Here, $\Omega_p = 0.005\gamma$ and $\Delta_p \approx 0$, whereas the remaining parameters are the same as those in Fig. 2(a).

increases then two or more than two photons per SA induce excitation, which creates absorption in the system. Whenever, Σ_{RR} approaches 1, then the three-level cascade atomic configuration reduces to the two-level atomic system as the vdW interaction goes to its maximum value. The strength of the vdW interaction is directly dependent on the input-probe-field intensity. To see the influence of vdW interactions on the EIG, we plot the central and first-order diffraction intensities versus s, as shown in Fig. 5. It is clear from the results that the diffraction intensity is high for small values of the vdW shift (s) and decreases exponentially when the vdW shift increases. This is due to the fact that the medium behaves like an EIT medium for a small vdW shift, but converts to a two-level atomic system when the vdW shift goes to its maximum value.

V. CONCLUSION

The realization of EIG using the concept of Rydberg blockade is important because Rydberg blockade makes the medium nonlinear and experimentally more viable. The Rydberg blockade effect, which is due to the vdW-induced shift, is directly related to the total population of the Rydberg states Σ_{RR} and it is well known that Σ_{RR} depends on the input probe field. Therefore, in the absence of vdW interaction inside the medium, i.e., no vdW-induced shift, $s(r) = 0$ and the medium becomes independent of the input-probe field.

The atom-field system with Rydberg excitations can exhibit EIT phenomena. Based on this fact, we have considered an atomic medium which consists of three-level cascade configuration with Rydberg excitations to realize atomic grating in the presence of the dipole blockade mechanism; we termed it the EIG via Rydberg atoms. We have investigated the role of the control field and the probe field to obtain maximum first-order diffraction intensity. We have observed that EIG is suppressed in atomic Rydberg states due to collective Rydberg excitations of SAs which depend upon the local input-probe-field intensity. Therefore, for small values of the probe-field intensity, the diffraction intensity increases while it decreases for the strong input field. This is due to the fact that for high intensity of the probe field, there exists more than one photon per SA and the excess photons are subjected to enhanced absorption of two-level atoms. The addition of two-photon correlations is the key characteristic of absorption of strong probe-field light. This absorption of the probe field leads to deterioration of the performance of the atomic grating.

We have also noticed that to obtain maximum diffraction intensity the control field also plays a role and relatively high intensity can be obtained for a relatively large control-field intensity. It is clear that the absorption of the probe field can be suppressed in the presence of strong control-field intensity and, therefore, slightly higher intensity in the first-order diffraction can be obtained via the control field even in the presence of a relatively large probe field. However, the overall behavior remains the same for all curves; i.e., after attaining the maximum value it decreases with a further increase in the probe-field Rabi frequency. We have also studied the dependence of diffraction intensity on the vdW interactions and observed that diffraction intensity can be higher for small vdW interactions, i.e., small vdW shift (s), and it decreases exponentially when the vdW interactions (shifts) increase. This is due to the fact that the medium behaves like an EIT medium for small vdW shifts, however, it is converted into a two-level atomic system when the vdW shifts become large.

In most practical implementations, SA models with Rydberg excitations have a lot of significance. Our proposed model not only provides an opportunity to realize background-free atomic grating but also, due to Rydberg atoms, provides a solution for practical implementation in quantum imaging and signal processing at a microscopic scale. Further, the control of the diffracted light can be achieved simply via the probe field and we can increase or decrease the diffracted light intensity using control of the probe field. We feel that the analysis presented here may provide a direction for the applications of atomic grating with Rydberg excitations which provide strong long-range atom-atom interactions.

[1] M. O. Scully and M. S. Zubairy, *Quantum Optics* (Cambridge University, Cambridge, England, 1997).
[2] S. E. Harris, Phys. Today **50**(7), 36 (1997).
[3] M. Fleischhauer, A. Imamoglu, and J. P. Marangos, Rev. Mod. Phys. **77**, 633 (2005).
[4] M. D. Lukin and A. Imamoglu, Phys. Rev. Lett. **84**, 1419 (2000).
[5] M. Yan, E. G. Rickey, and Y. F. Zhu, Opt. Lett. **26**, 548 (2001).
[6] M. D. Lukin and A. Imamoglu, Nature (London) **413**, 273 (2001).
[7] H. Y. Ling, Y.-Q. Li, and M. Xiao, Phys. Rev. A **57**, 1338 (1998).
[8] M. Mitsunaga and N. Imoto, Phys. Rev. A **59**, 4773 (1999).
[9] Luís E. E. de Araujo, Opt. Lett. **35**, 977 (2010).
[10] Z.-H. Xiao, S. G. Shin, and K. Kim, J. Phys. B: At. Mol. Opt. Phys. **43**, 161004 (2010).
[11] A. W. Brown and M. Xiao, Opt. Lett. **30**, 699 (2005).
[12] M. Bajcsy, A. S. Zibrov, and M. D. Lukin, Nature (London) **426**, 638 (2003).
[13] D. Moretti, D. Felinto, J. W. R. Tabosa, and A. Lezama, J. Phys. B **43**, 115502 (2010).
[14] B. K. Dutta and P. K. Mahapatra, J. Phys. B **39**, 1145 (2006).
[15] R. G. Wan, J. Kou, L. Jiang, Y. Jiang, and J. Y. Gao, Phys. Rev. A **83**, 033824 (2011).

[16] F. X. Zhou, Y. H. Qi, H. Sun, D. J. Chen, J. Yang, Y. P. Niu, and S. Q. Gong, Opt. Express **21**, 12249 (2013).
[17] Y. H. Qi, Y. P. Niu, Y. Xiang, H. L. Wang, and S. Q. Gong, Opt. Commun. **284**, 276 (2011).
[18] Z. H. Xiao, L. Zheng, and H. Lin, Opt. Express **20**, 1219 (2012).
[19] S. Q. Kuang, C. S. Jin, and C. Li, Phys. Rev. A **84**, 033831 (2011).
[20] L. Wang, F. X. Zhou, P. D. Hu, Y. P. Niu, and S. Q. Gong, J. Phys. B **47**, 225501 (2014).
[21] T. F. Gallagher, *Rydberg Atoms* (Cambridge University, Cambridge, England, 1994).
[22] J. D. Pritchard, D. Maxwell, A. Gauguet, K. J. Weatherill, M. P. A. Jones, and C. S. Adams, Phys. Rev. Lett. **105**, 193603 (2010).
[23] A. K. Mohapatra, T. R. Jackson, and C. S. Adams, Phys. Rev. Lett. **98**, 113003 (2007).
[24] A. K. Mohapatra *et al.*, Nat. Phys. **4**, 890 (2008).
[25] A. Tauschinsky, R. M. T. Thijssen, S. Whitlock, H. B. van Linden van den Heuvell, and R. J. C. Spreeuw, Phys. Rev. A **81**, 063411 (2010).
[26] M. D. Lukin, M. Fleischhauer, R. Cote, L. M. Duan, D. Jaksch, J. I. Cirac, and P. Zoller, Phys. Rev. Lett. **87**, 037901 (2001).
[27] D. Jaksch, J. I. Cirac, P. Zoller, S. L. Rolston, R. Côté, and M. D. Lukin, Phys. Rev. Lett. **85**, 2208 (2000).
[28] E. Urban, T. A. Johnson, T. Henage, L. Isenhower, D. D. Yauvz, T. G. Walker, and M. Saffman, Nat. Phys. **5**, 110 (2009); A. Gaëtan, Y. Miroshnychenko, T. Wilik, A. Chotia, M. Viteau, D. Comparat, P. Pillet, A. Browaeys, and P. Grangier, *ibid.* **5**, 115 (2009).
[29] T. Vogt, M. Viteau, J. Zhao, A. Chotia, D. Comparat, and P. Pillet, Phys. Rev. Lett. **97**, 083003 (2006).
[30] J. Honer, R. Low, H. Weimer, T. Pfau, and H. P. Buchler, Phys. Rev. Lett. **107**, 093601 (2011).
[31] J.-F. Huang, J.-Q. Liao, and C.-P. Sun, Phys. Rev. A **87**, 023822 (2013).
[32] D. Petrosyan, J. Otterbach, and M. Fleischhauer, Phys. Rev. Lett. **107**, 213601 (2011).
[33] Y.-M. Liu, D. Yan, X.-D. Tian, C.-L. Cui, and J.-H. Wu, Phys. Rev. A **89**, 033839 (2014).